The influence of spatial variability of soil permeability on the risk of rainfall induced landslides

J. Huang, A. Ali, A.V. Lyamin, S.W. Sloan
The University of Newcastle, Newcastle, Australia

D.V. Griffiths
Colorado School of Mines, Golden, USA

M. J. Cassidy, J. Li
The University of Western Australia, Perth, Australia

ABSTRACT: Rainfall induced landslides can vary in depth and deeper the landslide, greater is the damage it causes. This paper investigates, quantitatively, the risk of rainfall induced landslides by assessing the consequence of each failure. The influence of the spatial variability of the saturated hydraulic conductivity on the risk of landslides is studied. It is shown that a critical spatial correlation length exists at which the risk is a maximum.

1 INTRODUCTION

Landslides cause damage to buildings, infrastructure, agricultural land and crops. In the majority of cases the main trigger for landslides is heavy or prolonged rainfall (Brand 1984, Fourie 1996). The fundamental aspects connecting the hydrological and geotechnical processes that cause slope failure have been a subject of intensive research for many years. Previous research indicates that, rainfall-induced slope failures occur in initially unsaturated soil slopes, where, matric suction contributes to soil strength and, ultimately the slope stability (Rahardjo et al. 1995, Fredlund & Rahardjo 1993). During rainfall, saturated hydraulic conductivity controls the infiltration process, thereby, affecting the matric suction distribution, the soil strength and ultimately, the stability of the slope. Therefore, it is a very important factor that influences the stability of a slope during rainfall (Tsaparas et al. 2002, Rahardjo et al. 2007, Rahimi et al. 2010).

Most studies involving rainfall-induced landslides are deterministic in nature, where the soil is assumed to be homogeneous and averaged (or design) soil properties are considered in the analysis (Gui et al. 2000). Although few studies have focused on the effects of the spatial variability of the hydraulic conductivity on rainfall infiltration and subsequent slope stability by using random field theory (e.g. Santoso et al. 2011, Zhu et al. 2013, Cho 2014), none of them have investigated the nature of the triggering mechanism or quantified the risk associated with a rainfall-induced landslide.

It is now commonly believed that there are two mechanisms that trigger failure in slopes subject to rainfall infiltration (Li et al. 2013); loss of suction during propagation of the wetting front and the rise of the water table (which generates a positive pore water pressure). Despite decades of extensive studies on rainfall-induced landslides, the fundamental processes which trigger slope failure when the saturated hydraulic conductivity varies spatially are still not well quantified. Generally speaking, a loss of suction causes a shallow failure while a rise in the water table (i.e. generation of a positive pore water pressure) causes a deep failure. However, this may not be true when the saturated hydraulic conductivity varies spatially, as the water may accumulate at shallow depths (Huang et al. 2010) leading to a positive pore water pressure and a shallow failure. To the authors' knowledge, this important effect has not been studied systematically.

Another key aspect of the risk assessment of rainfall-induced landslides is the assessment of consequence. Rainfall-induced landslides can be shallow or deep. It is clear that a deep-seated landslide will tend to cause more damage and thus has a more severe consequence. Therefore, the consequence associated with a shallow or deep failure should be assessed individually. In this study, the saturated hydraulic conductivity of soil is modelled by random field theory and the risk of rainfall induced landslides is assessed based on the quantitative risk assessment framework proposed by Huang et al. (2013). The triggering mechanism of rainfall induced slope failure is also studied.

Landslides are characterized as failures occurring along a plane parallel to the ground surface. Given the physics involved in landslides, various infinite slope models have been used to assess their stability after heavy rainfall (e.g. Iverson 2000, Tsai 2008,

White & Singham 2012, Zhan et al. 2012, Li et al. 2013).Though the use of an infinite slope model requires certain assumptions (i.e. each slice of an infinitely long slope receives the same amount and intensity of rainfall; the time required for infiltration normal to the slope is much less than the infiltration time required for flow parallel to the slope; the wetting front propagates in a direction normal to the slope; and the depth of failure is small compared to the length of the failing soil mass), the validity of these assumptions has been checked against the predictions of two-dimensional numerical models, with the conclusion that an infinite slope approximation may be adopted as a simplified framework to assess failures due to the infiltration of rainfall (Li et al. 2013, Zhan et al. 2012). The present study is thus based on an infinite slope model.

In this study, the landslide risk of a hypothetical slope, where, only the saturated hydraulic conductivity varies spatially is investigated. The saturated hydraulic conductivity is modelled as a random field and coupled with Monte-Carlo simulations for the determination of failure probability, consequence and risk. To obtain the pore water distributions, the modified form of one-dimensional Richards equation (Richards 1931) is solved numerically by the HYDRUS 1D software (Simunek et al. 2013).

2 SEEPAGE ANALYSIS

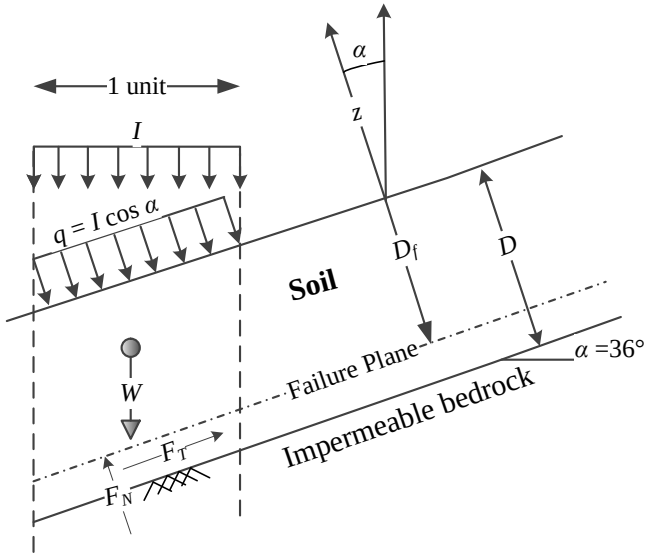

Figure 1. Geometry and limit equilibrium set-up.

Assuming that the effect of pore-air pressure is insignificant and that water flow due to thermal gradients is negligible, one-dimensional uniform flow in a variably saturated soil can be described by a modified form of Richards equation (Richards 1931). Therefore, the flow in an unsaturated infinite soil slope can be described by the one-dimensional equation (e.g. Zhan et al. 2012):

$$\frac{d\theta}{dt} = \frac{d}{dz}\left(K\left[\frac{du}{dz} + \cos\alpha \right] \right) \tag{1}$$

where θ is the volumetric water content, t is time, u is the pore water pressure head, α is the inclination of the slope to the horizontal, K is the hydraulic conductivity and z is the spatial coordinate as shown in Figure 1. To solve the above equation numerically, the water content θ is assumed to vary with the pore water pressure head, u, according to the van Genuchten (1980) model as:

$$S_e = \frac{\theta - \theta_r}{\theta_s - \theta_r} = \left[\frac{1}{1 + (au)^N} \right]^m \tag{2}$$

where S_e is the effective degree of saturation, θ_s and θ_r are the saturated and residual water content respectively, a is the suction scaling parameter and N, m are the parameters of the van Genuchten model. To complete the description, the hydraulic conductivity K can be estimated as:

$$K = K_s K_r \tag{3}$$

where K_s is the saturated hydraulic conductivity and K_r is the relative hydraulic conductivity given by van Genuchten (1980):

$$K_r = S_e^{1/2}[1 - (1 - S_e^{1/m})^m]^2 \tag{4}$$

In this study, the saturated hydraulic conductivity is modelled as a random field and Equation 1 is solved by HYDRUS 1D. The distribution of pore water pressure and the degree of saturation are then used in the infinite slope model to assess the slope stability.

2.1 *Slope stability*

Once the pore water pressure distribution is obtained through seepage analysis, the factor of safety FS at any given time t can then be determined by limit-equilibrium techniques. The stability of an infinite slope is estimated by using a closed form solution similar to that proposed by White & Singham (2012), where the failure is considered to occur along a plane parallel to the ground surface. A soil column of a unit width is considered, where the self-weight W is used to obtain the normal force F_N and tangential force F_T at any depth. The expression for the factor of safety is similar to that considered by White & Singham (2012). The only difference being that, instead of using saturation (S) weighted suction stress, the effective degree of saturation (S_e) weighted suction stress is considered.

The factor of safety FS was analyzed using the expression:

$$FS = \frac{\tan\phi'}{\tan\alpha} + \frac{c' - S_e u_w \tan\phi'}{W \cos\alpha \sin\alpha} \tag{5}$$

where ϕ' is the effective friction angle, c' is the effective cohesion, u_w is the pore water pressure (= $u\gamma_w$). FS = 1 corresponds to a limiting condition for equilibrium, and failure occurs when FS is less than 1.

3 PROBABILISTIC ANALYSIS

3.1 *Random Field Theory*

Random fields are characterized by a distribution (e.g. log-normal type) and a spatial correlation structure. The present study considers the saturated hydraulic conductivity, K_s, to be log-normally distributed which is consistent with field measurements (Hoeksema & Kitanidis 1985, Sudicky 1986). A log-normal distribution can be easily arrived at by a non-linear transformation of the normal (Gaussian) distribution and it ensures that the random variable is always positive (Griffiths et al. 2011). Such a distribution has also been used by several investigators for modelling saturated hydraulic conductivity statistically (e.g. Santoso et al. 2011, Zhu et al. 2013, Cho 2014). A log-normally distributed K_s is defined by two parameters, a mean (μ_{K_s}) and coefficient of variation (ν_{K_s}) which are related by:

$$\nu_{K_s} = \frac{\sigma_{K_s}}{\mu_{K_s}} \tag{6}$$

where σ_{K_s} is the standard deviation for the log-normally distributed K_s. The equivalent parameters of the normally distributed lnK_s- $\mu_{\ln K_s}$ and $\sigma_{\ln K_s}$ (i.e. the mean and standard deviation of lnK_s) are:

$$\sigma^2_{\ln K_s} = \ln(1+\nu^2_{K_s}) \tag{7}$$

$$\mu_{\ln K_s} = \ln(\mu_{K_s}) - \frac{1}{2}\sigma^2_{\ln K_s} \tag{8}$$

In addition to the mean and the coefficient of variation, a third parameter, the spatial correlation length $\theta_{\ln K_s}$, is required to completely define a random field. The spatial correlation length defines the distance over which the soil properties are significantly correlated; with properties separated by a distance greater than $\theta_{\ln K_s}$ being generally uncorrelated. A large spatial correlation length means that the soil properties are highly correlated over a large distance, implying less spatial variability and more uniformity in soil properties. Conversely, a small correlation length implies a higher spatial variability and less uniformity in the soil properties. In the context of random fields, the spatial correlation lengths are generally incorporated through a correlation function. The correlation function ρ assumed for the present study is an exponential one of the form:

$$\rho(z) = \exp\left(-\frac{|z|}{\theta_{\ln K_s}}\right) \tag{9}$$

Based on the log-normal distribution and the correlation function defined above, one-dimensional random fields for saturated hydraulic conductivity K_s can be generated. In the present study, the Karhunen Loève (KL) expansion method (Zhang & Lu 2004) is used for this purpose. Note that the required number of terms in the KL expansion increases when the spatial correlation length decreases and, for the smallest $\theta_{\ln K_s}$ considered in this study, more than 5000 terms were used. The Karhunen Loève expansion method generates a Gaussian (normal) random field and K_s being log-normal, requires a log-normal random field. This is obtained through the transformation:

$$K_{sj} = \exp(\mu_{\ln K_s} + \sigma_{\ln K_s} \times g_j) \tag{10}$$

where K_{sj} is the saturated hydraulic conductivity assigned to the j^{th} node (of the one-dimensional finite element mesh) and g_j is the Gaussian equivalent of K_{sj} obtained from a zero mean and unit standard deviation. The dimensionless form of spatial correlation length Θ is defined as:

$$\Theta = \frac{\theta_{\ln K_s}}{D} \tag{11}$$

where D is the length of the random field.

3.2 *Risk assessment*

During rainfall, water infiltrates into the soil from the top and can cause shallow or deep failures. It is clear that a deep failure will tend to cause more damage and thus has a more severe consequence. Therefore, the consequence associated with shallow and deep failures should be assessed individually. In the present study, consequence is assumed to be directly related to the failure depth (D_f). The risk (R) is defined as:

$$R = \sum_{i=1}^{n_f} p_{fi} \times C_i \tag{12}$$

where p_{fi} and C_i are the probability and consequence of the i^{th} failure , and n_f is the number of failures. In applications (e.g. Cassidy et al. 2008), an additional vulnerability component would be added to Equation 12. However, it has been assumed to be one here for simplicity and to concentrate the paper on the novel developments. Equation 12 can be rewritten in the traditional form as:

$$R = \sum_{i=1}^{n_f} p_{fi} \times C_i = \sum_{i=1}^{n_f} \frac{1}{n_{sim}} \times C_i$$

$$= \frac{1}{n_{sim}} \sum_{i=1}^{n_f} C_i = \frac{n_f}{n_{sim}} \frac{\sum_{i=1}^{n_f} C_i}{n_f} \quad (13)$$

$$= p_f \times C$$

where C is the consequence and n_{sim} is the number of Monte-Carlo simulations.

$$p_f = \frac{n_f}{n_{sim}} \quad (14)$$

and

$$C = \frac{\sum_{i=1}^{n_f} C_i}{n_f} \quad (15)$$

It can be seen from Equation 15 that consequence (C) in the traditional risk definition should be redefined as the average consequence of all failures.

4 STUDY

In the present investigation, a hypothetical slope, at an inclination of α = 36° to the horizontal, is considered as shown in Figure 1. A 1m thick soil layer (having the mechanical and hydraulic properties shown in Table 1) is considered to be underlain by rock (i.e. D = 1 m). The water table is initially 2m (all distances measured normal to the slope i.e. along "*z*" direction) below the ground surface and is assumed to be constant throughout the analysis. The initial pore water pressure profile is hydrostatic and, as rainfall occurs, the water is assumed to infiltrate in a wetting front normal to the slope. The rainfall intensity is $I = 0.25\mu_{K_s}$, and the flux q infiltrating the soil at the top is $I\cos\alpha$. No ponding of water is allowed at the ground surface at any time. Based on the expression for the factor of safety (Equation 5) with the parameters described in Table 1 and considering α = 36°, the factor of the safety before rainfall (considering a hydrostatic distribution) is 1.285.

In order to investigate the effect of the spatial variability of the saturated hydraulic conductivity K_s on landslides risk, K_s is modelled as a log-normal stationary random field while other parameters are deterministic. The probability of failure (p_f), consequence (C), and risk (R) associated with rainfall-induced failure of the purely frictional soil slope (i.e. c' = 0) is investigated. From the literature it is observed that the saturated hydraulic conductivity varies in the range of ν_{K_s} = 0.6 to 0.9 (Duncan 2000). Taking the higher end of the range for the random field study, ν_{K_s} = 1 is considered. Table 2 summarizes the parameters for the random field study. Two thousand Monte Carlo simulations were conducted for each spatial correlation length. For each realization of the random field of K_s, seepage analysis is performed for a duration equal to the time, when the slope would fail with deterministic K_s = μ_{K_s}. The pore water pressure results are then used to perform slope stability analysis.

Table 1. Material properties of the soil (White & Singham 2012)

Parameter	Symbol	Value	Units
Porosity	n	0.40	
Unit weight of soil	γ_s	20	kN/m^3
Unit weight of water	γ_w	10	kN/m^3
Mean saturated hydraulic conductivity	μ_{K_s}	8.64	m/day
Residual water content	θ_r	0.128	
Saturated water content	θ_s	0.40	
Scaling suction	a	5.00	1/m
Van Genuchten model parameter	N	1.5	
Van Genuchten model parameter	m	1−1/N	
Effective cohesion	c'	0	kPa
Effective friction angle	ϕ'	35	degrees

Table 2. Parameters for the probabilistic study.

Parameter	Symbol	Value	Units
Coefficient of variation of saturated hydraulic conductivity	ν_{K_s}	1	
Spatial correlation length	Θ	0.125,0.25, 0.50, 1.00, 2.00, 8.00, 100	
Length of random field	D	1	m
Number of simulations	n_{sim}	2000	

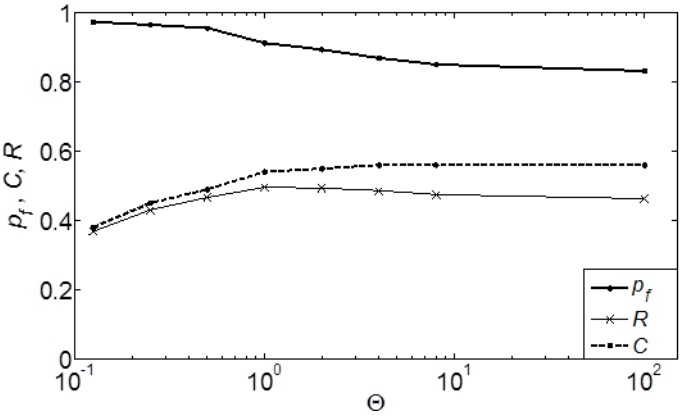

Figure 2. Variation in probability of failure, consequence and risk.

The variation in the probability of failure (p_f), consequence (C) and risk (R) with the spatial corre-

lation length (Θ) is shown in Figure 2. The smallest correlation length (Θ = 0.125), has the greatest spatial variability (in this study) and it results in the highest probability of failure (p_f) and the lowest consequence. With an increase in spatial correlation length (the soil becomes more uniform,) p_f decreases and C increases. On the other hand, the risk reaches its maximum when Θ is equal to the depth of the slope i.e. Θ = 1.0. This highlights the importance of individual assessment of the failure consequence.

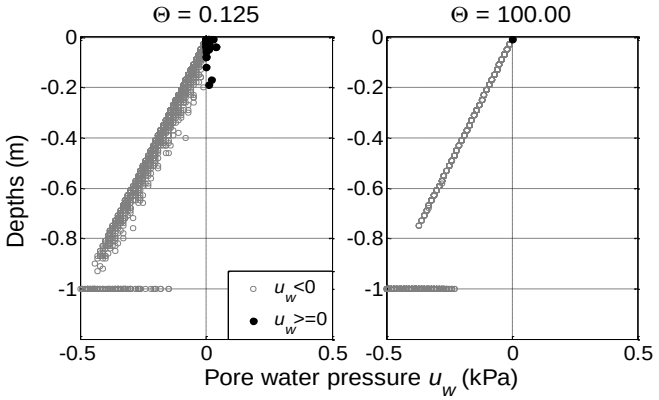

Figure 3. Scatter plot of pore water pressure at failure for different spatial correlation lengths.

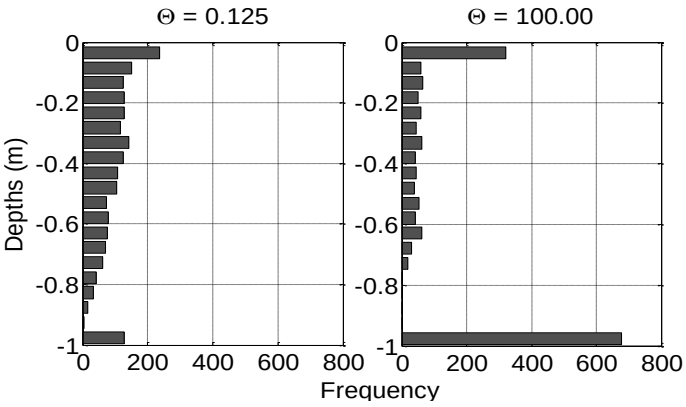

Figure 4. Histogram of failure depths for different spatial correlation lengths.

Figure 3 shows a scatter plot of the pore water pressure u_w at failure, plotted against the corresponding failure depths, for two extreme values of the spatial correlation length Θ: 0.125 and 100. The solid points represent failures due to the generation of positive pore water pressures while the hollow points represent failures due to loss of suction. Firstly, the greatest scattering can be observed in the distribution of pore water pressure at failure when the spatial correlation length Θ is small. At large spatial correlation lengths, the scatter in pore water pressure is less. Secondly, at smaller correlation lengths though most of the failures are due to loss of suction, slope failure may also occur due to the generation of positive pore water pressures as shown by the solid points. This could be attributed to non-uniformity in the weight of the failing soil mass W. The weight W is obtained by integrating the unit weight γ throughout the depth to account for variations in the water content. So, at a smaller Θ, there is more non-uniformity (or randomness) in the weight W throughout the depth, thus requiring a greater reduction in the pore water pressure to cause failure.

Figure 4 shows the histogram of failure depths for different spatial correlation length and it can be used to understand the results observed in Figure 2. When spatial correlation length is small, there are a large number of shallow failures (i.e. failures above the boundary) and few deep failures (i.e. failures occurring at the boundary). Now, as the spatial correlation length increases, the soil becomes more uniform. Obviously, if there are more shallow failures, the probability of failure will also be high. Also, if failures are shallow, the consequence will be low while if the failures are deep the consequence will be high. This explains why, the probability of failure was initially high, and then decreased with an increase in spatial correlation length; and why consequence was initially low and then increased with an increase in spatial correlation length.

5 CONCLUSIONS

The risk of rainfall induced landslides was studied quantitatively, based on the logic that the consequence should be assessed individually for each failure. When the saturated hydraulic conductivity was modelled as a random field, it was shown that the probability of failure increases as the spatial correlation length increases. However, when consequence of failure (measured here by the depth of the failure) was accounted for, a critical spatial correlation length exists at which the risk was maximum. This confirms clearly that the consequence should be assessed individually for a rational risk assessment. The triggering mechanism for a rainfall induced landslide was also highlighted by the pore water pressure distributions at failure. For small spatial correlation lengths, water can accumulate at shallow depths thereby generating positive pore water pressures which are sufficient to cause shallow failures.

REFERENCES

Brand, E. W. (1984) Landslides in South Asia: a state-of-art report. *4th International Symposium on Landslides, Toronto.*

Cassidy, M. J.,Uzielli, M. & Lacasse, S. (2008) Probability risk assessment of landslides: a case study at Finneidfjord. *Canadian Geotechnical Journal,* 45**,** 1250-1267.

Cho, S. E. (2014) Probabilistic stability analysis of rainfall-induced landslides considering spatial variability of permeability. *Engineering Geology,* 171**,** 11-20.

Duncan, J. M. (2000) Factors of safety and reliability in geotechnical engineering. *Journal of Geotechnical and Geoenvironmental Engineering,* 126**,** 307-316.

Fourie, A. B. (1996) Predicting rainfall-induced slope instability. *Proceedings of the ICE-Geotechnical Engineering,* 119**,** 211-218.

Fredlund, D. G. & Rahardjo, H. (1993) *Soil mechanics for unsaturated soils,* New York, John Wiley & Sons, Inc.

Griffiths, D. V.,Huang, J. & Fenton, G. A. (2011) Probabilistic infinite slope analysis. *Computers and Geotechnics,* 38**,** 577-584.

Gui, S.,Zhang, R.,Turner, J. P. & Xue, X. (2000) Probabilistic slope stability analysis with stochastic soil hydraulic conductivity. *Journal of Geotechnical and Geoenvironmental Engineering,* 126**,** 1-9.

Hoeksema, R. J. & Kitanidis, P. K. (1985) Analysis of the spatial structure of properties of selected aquifers. *Water Resources Research,* 21**,** 563-572.

Huang, J.,Griffiths, D. V. & Fenton, G. A. (2010) Probabilistic analysis of coupled soil consolidation. *Journal of Geotechnical and Geoenvironmental Engineering,* 136**,** 417-430.

Huang, J.,Lyamin, A. V.,Griffiths, D. V.,Krabbenhøft, K. & Sloan, S. W. (2013) Quantitative risk assessment of landslide by limit analysis and random fields. *Computers and Geotechnics,* 53**,** 60-67.

Iverson, R. M. (2000) Landslide triggering by rain infiltration. *Water Resources Research,* 36**,** 1897-1910.

Li, W. C.,Lee, L. M.,Cai, H.,Li, H. J.,Dai, F. C. & Wang, M. L. (2013) Combined roles of saturated permeability and rainfall characteristics on surficial failure of homogeneous soil slope. *Engineering Geology,* 153**,** 105-113.

Rahardjo, H.,Lim, T. T.,Chang, M. F. & Fredlund, D. G. (1995) Shear-strength characteristics of a residual soil. *Canadian Geotechnical Journal,* 32**,** 60-77.

Rahardjo, H.,Ong, T.,Rezaur, R. & Leong, E. (2007) Factors controlling instability of homogeneous soil slopes under rainfall. *Journal of Geotechnical and Geoenvironmental Engineering,* 133**,** 1532-1543.

Rahimi, A.,Rahardjo, H. & Leong, E. C. (2010) Effect of hydraulic properties of soil on rainfall-induced slope failure. *Engineering Geology,* 114**,** 135-143.

Richards, L. A. (1931) Capillary conduction of liquids through porous mediums. *Physics,* 1**,** 318-333.

Santoso, A. M.,Phoon, K. K. & Quek, S. T. (2011) Effects of soil spatial variability on rainfall-induced landslides. *Computers & Structures,* 89**,** 893-900.

Simunek, J.,van Genuchten, M. T. & Sejna, M. (2013) The Hydrus-1D software package for simulating the movement of water, heat, and multiple solutes in variably saturated media, Version 4.16, HYDRUS Software Series 3. Department of Environmental Sciences, University of California Riverside, Riverside, California, USA.

Sudicky, E. A. (1986) A natural gradient experiment on solute transport in a sand aquifer: spatial variability of hydraulic conductivity and its role in the dispersion process. *Water Resources Research,* 22**,** 2069-2082.

Tsai, T. L. (2008) The influence of rainstorm pattern on shallow landslide. *Environmental Geology,* 53**,** 1563-1569.

Tsaparas, I.,Rahardjo, H.,Toll, D. G. & Leong, E. C. (2002) Controlling parameters for rainfall-induced landslides. *Computers and Geotechnics,* 29**,** 1-27.

van Genuchten, M. T. (1980) A closed-form equation for predicting the hydraulic conductivity of unsaturated soils. *Soil Science Society of America Journal,* 44**,** 892-898.

White, J. A. & Singham, D. I. (2012) Slope stability assessment using stochastic rainfall simulation. *Procedia Computer Science,* 9**,** 699-706.

Zhan, T. L. T.,Jia, G. W.,Chen, Y. M.,Fredlund, D. G. & Li, H. (2012) An analytical solution for rainfall infiltration into an unsaturated infinite slope and its application to slope stability analysis. *International Journal for Numerical and Analytical Methods in Geomechanics,* 37**,** 1737–1760.

Zhang, D. & Lu, Z. (2004) An efficient, high-order perturbation approach for flow in random porous media via Karhunen–Loève and polynomial expansions. *Journal of Computational Physics,* 194**,** 773-794.

Zhu, H.,Zhang, L. M.,Zhang, L. L. & Zhou, C. B. (2013) Two-dimensional probabilistic infiltration analysis with a spatially varying permeability function. *Computers and Geotechnics,* 48**,** 249-259.